ACS Photonics

Article

pubs.acs.org/journal/apchd5

Resonant Thermal Infrared Emitters in Near- and Far-Fields

Baoan Liu, Jiayu Li, and Sheng Shen*

Department of Mechanical Engineering, Carnegie Mellon University, Pittsburgh, Pennsylvania 15213, United States

ABSTRACT: Although optical resonators are widely used for controlling and engineering thermal radiation, what has been lacking is a general theoretical framework to elucidate the thermal emission of optical resonators. We developed a general and self-consistent formalism to describe the thermal radiation from arbitrary optical resonators made by lossy and dispersive materials like metals, with the only assumption that the resonators have a single predominant resonance mode. Our formalism derives the fundamental limit of the spectral thermal emission power from an optical resonator and proves that this limit can be achieved when the mode losses to the emitter and the absorber (or far-field background) are matched, and meanwhile, the predominant resonant mode is electrically quasi-static. By efficiently calculating the resonant modes using the finite element methods, our formalism serves as a general principle of designing the arbitrary optical resonator thermal emitters with perfect or maximized emission in both near- and far-fields.

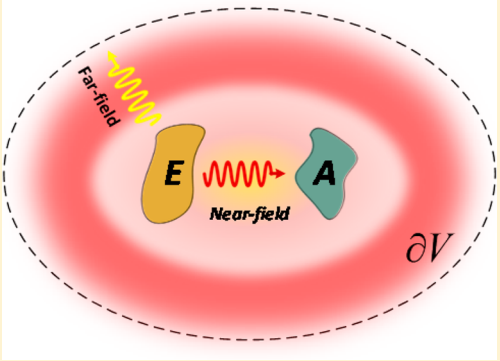

KEYWORDS: *Quasi-Normal Mode theory, fluctuational electrodynamics, near- and far-field thermal radiation, metamaterials, perfect emission*

A thermal light source like a blackbody or the incandescent filament of a light bulb usually has a broad emission spectrum. However, in many applications such as infrared sensing,[1] thermophotovoltaics,[2,3] radiation cooling,[4] and thermal circuits,[5,6] thermal emission is in general required to be much narrower than that of a blackbody. A common paradigm for realizing narrow band thermal radiation is to utilize optical resonators including optical antennas,[7] resonant metamaterials,[8] photonic crystal cavities,[9] graphene nanostructures,[6,10] and so on. According to the Purcell effect,[11] thermal radiation from an optical resonator can be dramatically modulated by the resonance mode designed in the infrared range, leading to the narrow band thermal emission at the resonant frequency. On the other hand, since thermal radiation is intrinsically weaker than the infrared light from light sources driven by electrical power, for example, laser or LED, it is critical to maximize the emission power of an optical resonator.

Here, we develop a general and self-consistent formalism from fluctuational electrodynamics[12] and Quasi-Normal Mode (QNM) theory[13−15] to describe the thermal radiation from optical resonators with arbitrary geometries that are made by lossy and dispersive materials like metals. By only assuming an optical resonator with a single predominant resonance mode, our formalism derives the fundamental limit of the spectral thermal emission power from an optical resonator and proves that this limit can be achieved when the mode losses to the emitter and the absorber (or far-field background) are matched, and meanwhile, the resonance mode is electrically quasi-static, that is, the electric field oscillates in phase. The new theoretical framework developed in this work is intrinsically different from previous phenomenological approaches based on the Coupled-Model Theory (CMT),[5,9,16,17] in which a resonant thermal emitter is simplified as a generic resonant system with two lumped impedances describing the mode losses inside the emitter and to an absorber, respectively. Although the CMT states that the thermal emission power is maximized when the two impedances are matched, the most critical concept of "impedance" or "mode loss" in the CMT does not have an electromagnetic definition, and can only be treated as fitting parameters instead.[5,9,17] In contrast, our formalism provides a rigorous electromagnetic definition to the mode loss in terms of the mode field profile, which has a closed-form expression by considering the non-Hermitian nature of the lossy resonant mode and the material dispersion.

RESULTS AND DISCUSSION

Theory. Consider a thermal emitter V_E at the temperature of T_E and a closely separated object V_A, where V_E and V_A are placed in vacuum, as shown in Figure 1. Here, we assume that the materials are nonmagnetic, and have isotropic electrical responses. Since the thermal radiation from V_E is physically the emission of electromagnetic waves $[\mathbf{E}(r, \omega), \mathbf{H}(r, \omega)]$ generated by the thermally induced random currents $\mathbf{j}(r, \omega, T_E)$ inside V_E, the spectral thermal energy transfer from V_E to V_A is therefore equal to the averaged electromagnetic absorption power of V_A,

$$\phi_A(\omega) = \int_{V_A} dr^3 \left\langle \frac{1}{2}\sigma_A \mathbf{E}(r, \omega)^{\dagger} \cdot \mathbf{E}(r, \omega) \right\rangle \quad (1)$$

Received: March 31, 2017
Published: May 18, 2017

DOI: 10.1021/acsphotonics.7b00336
ACS Photonics 2017, 4, 1552−1557

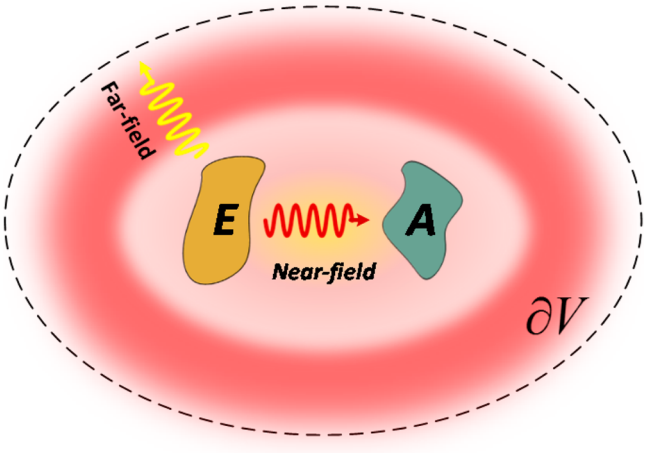

Figure 1. Schematic of a thermal emitter and a near-field absorber placed in the vacuum background.

where † denotes the conjugate-transpose, both the field and the current are expressed as 3-by-1 column vectors, and σ indicates the electric conductivity of a material, which relates to its permittivity as $\sigma(\omega) = \omega\mathrm{Im}[\epsilon(\omega)]$. Similarly, the spectral energy transfer from V_E to the far-field, $\phi_\infty(\omega)$, equals the integration of the averaged Poynting vector over an enclosure surface ∂V, which can be further expressed by the total power from the current sources minus the near-field power absorption in both V_E and V_A according to energy conservation,[18]

$$\begin{aligned}\phi_\infty(\omega) &= \int_{\partial V} \mathrm{d}r^2 \hat{\mathbf{n}}\cdot\left\langle \frac{1}{2}\mathrm{Re}[\mathbf{E}\times\mathbf{H}^\dagger]\right\rangle \\ &= -\int_{V_\mathrm{E}} \mathrm{d}r^3\left\langle \frac{1}{2}\mathrm{Re}[\mathbf{j}^\dagger\cdot\mathbf{E}]\right\rangle - \int_{V_\mathrm{E}} \mathrm{d}r^3\left\langle \frac{1}{2}\sigma_\mathrm{E}|\mathbf{E}|^2\right\rangle \\ &\quad - \int_{V_\mathrm{A}} \mathrm{d}r^3\left\langle \frac{1}{2}\sigma_\mathrm{A}|\mathbf{E}|^2\right\rangle \end{aligned} \tag{2}$$

where $|\mathbf{E}|^2 = \mathbf{E}^\dagger\cdot\mathbf{E}$. Note that we ignore the backward thermal radiation from both V_A and the background to V_E. In addition, the spectral energy transfer $\phi(\omega)$ relates to the total power Φ as $\Phi = \int_0^\infty \mathrm{d}\omega\phi(\omega)$.

The spectral energy transfer $\phi_\mathrm{A}(\omega)$ and $\phi_\infty(\omega)$ in eqs 1 and 2 can be formulated as deterministic expressions, because (i) the electric field emitted by the random currents can be represented as $\mathbf{E}(r,\omega) = i\omega\mu_0\int_{V_\mathrm{E}}\mathrm{d}r'^3\bar{\mathbf{G}}_{\omega,r,r'}\cdot\mathbf{j}(r',\omega,T_\mathrm{E})$, where $\bar{\mathbf{G}}_{\omega,r,r'}$ is the Dyadic Green's function defined as the impulse response of the wave equation $[\nabla\times\nabla\times + \omega^2\mu_0\epsilon(\omega,r)]\bar{\mathbf{G}}_{\omega,r,r'} = \bar{\mathbf{I}}\delta(r-r')$ and $\bar{\mathbf{I}}$ is the 3-by-3 unit matrix;[11] (ii) the autocorrelation of the random currents $\boldsymbol{j}(r,\omega,T_\mathrm{E})$ is characterized by the fluctuation−dissipation theorem[12] as

$$\langle\mathbf{j}(r,\omega,T_\mathrm{E})\mathbf{j}^\dagger(r',\omega,T_\mathrm{E})\rangle = \frac{4}{\pi}\sigma_\mathrm{E}\Theta(\omega,T_\mathrm{E})\delta(r-r')\bar{\mathbf{I}} \tag{3}$$

where $\Theta(\omega,T) = \hbar\omega/[\exp(\hbar\omega/k_\mathrm{B}T) - 1]$ is the Planck distribution. Substituting the Dyadic Green's function and eq 3 into eq 1, $\phi_\mathrm{A}(\omega)$ becomes

$$\phi_\mathrm{A}(\omega) = \frac{\Theta}{2\pi}4\omega^2\mu_0{}^2\mathrm{Tr}\left[\int_{V_\mathrm{A}}\mathrm{d}r^3\int_{V_\mathrm{E}}\mathrm{d}r'^3\sigma_\mathrm{A}\sigma_\mathrm{E}\bar{\mathbf{G}}^\dagger_{\omega,r,r'}\cdot\bar{\mathbf{G}}_{\omega,r,r'}\right] \tag{4}$$

where $\mathrm{Tr}[\cdot]$ denotes the trace of the matrix. Similarly, for the first term on the right-hand side of eq 2, we have $-\int_{V_\mathrm{E}}\mathrm{d}r^3\frac{1}{2}\mathrm{Re}[\mathbf{j}^\dagger\cdot\mathbf{E}] = \frac{\Theta}{2\pi}4\omega\mu_0\mathrm{Tr}[\int_{V_\mathrm{E}}\mathrm{d}r^3\sigma_E\mathrm{Im}[\bar{\mathbf{G}}_{\omega,r,r}]]$. Together with eq 4, $\phi_\infty(\omega)$ becomes

$$\begin{aligned}\phi_\infty(\omega) = \frac{\Theta}{2\pi}\{&4\omega\mu_0\mathrm{Tr}\left[\int_{V_\mathrm{E}}\mathrm{d}r^3\sigma_\mathrm{E}\mathrm{Im}[\bar{\mathbf{G}}_{\omega,r,r}]\right] \\ &- 4\omega^2\mu_0{}^2\mathrm{Tr}\left[\int_{V_\mathrm{E}}\mathrm{d}r^3\int_{V_\mathrm{E}}\mathrm{d}r'^3\sigma_\mathrm{E}^2\bar{\mathbf{G}}^\dagger_{\omega,r,r'}\cdot\bar{\mathbf{G}}_{\omega,r,r'}\right] \\ &- 4\omega^2\mu_0{}^2\mathrm{Tr}\left[\int_{V_\mathrm{A}}\mathrm{d}r^3\int_{V_\mathrm{E}}\mathrm{d}r'^3\sigma_\mathrm{A}\sigma_\mathrm{E}\bar{\mathbf{G}}^\dagger_{\omega,r,r'}\cdot\bar{\mathbf{G}}_{\omega,r,r'}\right]\}\end{aligned} \tag{5}$$

Equations 4 and 5 are the general expressions for near-field and far-field thermal radiation, respectively. The only assumption is the quasi-thermal equilibrium in V_E, that is, uniform temperature inside the emitter V_E.

If the thermal emitter in Figure 1 is simultaneously an optical resonator, its far-field and near-field thermal radiation can be narrow-band and modulated by a predominant resonant mode. In this scenario, we can expand the Dyadic Green's function $\bar{\mathbf{G}}_{\omega,r,r'}$ in terms of the resonant modes based on QNM theory, especially for dispersive and lossy materials. For an optical resonator in vacuum (as shown in Figure 1), its resonant modes are naturally defined as the eigen-solutions of the source-free Maxwell equations

$$\begin{aligned}\nabla\times\mathbf{E}_n(r) &= i\omega_n\mu_0\mathbf{H}_n(r) \\ \nabla\times\mathbf{H}_n(r) &= -i\omega_n\epsilon(\omega_n,r)\mathbf{E}_n(r)\end{aligned} \tag{6}$$

Here, the electromagnetic fields $[\mathbf{E}_n(r), \mathbf{H}_n(r)]$ satisfy the outgoing wave boundary condition at $|r|\to\infty$.[13,14] In eq 6, ω_n is the eigen-frequency, which is a complex number in the cases that the resonant mode is lossy. Specifically, $\mathrm{Re}[\omega_n]$ equals the resonant frequency, and $\mathrm{Im}[\omega_n]$ indicates the mode loss rate. Note that a thermal emitter has $\mathrm{Im}[\omega_n] < 0$ because it must contain dissipative materials to radiate, according to eq 3.

Since $\bar{\mathbf{G}}_{\omega,r,r'}$ is essentially the impulse response of the Maxwell equations, it can be mathematically expanded in terms of the eigen-solutions of the Maxwell equations, when the resonant modes are orthonormal and complete[19] as

$$\bar{\mathbf{G}}_{\omega,r,r'} = \sum_n \frac{\mathbf{E}_n(r)\cdot\mathbf{E}_n^\dagger(r')}{\omega\mu_0(\omega_n-\omega)N_{nn}} \tag{7}$$

where N_{nn} is the orthonormal factor for the mode n to itself. However, the orthonormality and completeness of the lossy resonant modes are difficult to be defined and justified. Until recently, this difficulty is resolved by QNM[13,14] theory. Since we are only interested in the frequencies in the vicinity of the resonant frequency of a predominated resonant mode, QNM theory proves that the orthonormality and completeness in this condition are approximately held by defining the orthonormal factor N_{nm}[14,20] as

$$N_{nm} = \int_{V_\infty}\mathrm{d}r^3\left[\frac{\partial\omega\epsilon(r,\omega)}{\partial\omega}\mathbf{E}_n^\mathrm{T}\cdot\mathbf{E}_m - \frac{\partial\omega\mu}{\partial\omega}\mathbf{H}_n^\mathrm{T}\cdot\mathbf{H}_m\right]\Bigg|_{\omega=\omega_n} \tag{8}$$

where X^T denotes the matrix transpose and V_∞ indicates the entire space. The "quasi-" completeness requires that (i) only the field inside or in proximity to the optical resonator can be expanded by the lossy resonant modes;[13,14] (ii) the lossy resonant modes used in the expansion account for all the important energy decay channels.[14] Both of these two

DOI: 10.1021/acsphotonics.7b00336
ACS Photonics 2017, 4, 1552−1557

requirements are satisfied in our cases, because (i) eqs 4 and 5 only evaluate $\bar{\mathbf{G}}_{\omega,r,r'}$ with $r, r' \in V_E \cup V_A$; (ii) the thermal emitters studied in our cases are assumed to have a predominant resonant mode. Furthermore, the "quasi-" orthonormality of the lossy resonant modes approximately holds for $\omega \approx \omega_n$. The QNM theory for expanding the field by using the lossy resonant modes has recently attracted massive attentions.[13] Several reports have demonstrated the good accuracy of QNM theory by comparing the directly simulated field profile $[\mathbf{E}(r, \omega), \mathbf{H}(r, \omega)]$ near the resonant structures emitted by a dipole source with the expansion of its lossy resonant modes, and good agreements are observed.[14,21,22] As a result, QNM theory justifies that eq 7 with the definition of N_{nn} in eq 8 is approximately held for the lossy resonant modes expansion near the resonant frequency $\omega \approx \mathrm{Re}[\omega_n]$, which can then be substituted into eqs 4 and 5.

To clarify the effect of an individual resonant mode on thermal radiation, we simplify the physics by assuming the nondegeneracy of the resonant modes, and their resonant frequencies $\mathrm{Re}[\omega_n]$ are highly distinct from each other. Consider the frequencies around the resonant frequency of the predominant resonant mode, that is, $\omega \approx \mathrm{Re}[\omega_n]$. The near-field radiative energy transfer from V_E to V_A in eq 4 becomes

$$\phi_A(\omega) = \frac{\Theta(\omega, T)}{2\pi}\left[\frac{\mathrm{Re}[\omega_n]^2}{\mathrm{Re}[\omega_n]^2 + 4Q_n^2(\mathrm{Re}[\omega_n] - \omega)^2}\right]\psi_A(\omega) = \frac{\Theta(\omega, T)}{2\pi}L(\omega)\psi_A(\omega) \tag{9}$$

where $L(\omega)$ is the Lorentzian line shape function with the peak at the resonant frequency $\omega = \mathrm{Re}[\omega_n]$, and $Q_n = \left|\frac{\mathrm{Re}[\omega_n]}{2\mathrm{Im}[\omega_n]}\right|$ is the Q-factor of the resonant mode n. It should be noted that our theory is also expected to provide correct description of the thermal radiation from multiple nondegenerate modes by summing up contributions from each of them in the $L(\omega)$ term. Equation 9 predicts the line shape of the peak in thermal radiation spectrum, where the peak width is inversely proportional to the quality factor Q_n, and the peak height is determined by $\psi_A(\omega)$ that can be expressed as

$$\psi_A(\omega) = \frac{16}{\mathrm{Im}[\omega_n]^2}\frac{1}{|N_{nn}|^2}\left[\int_{V_A} \mathrm{d}r^3 \frac{1}{2}\sigma_A(\omega)|\mathbf{E}_n(r)|^2\right] \times \left[\int_{V_E} \mathrm{d}r'^3 \frac{1}{2}\sigma_E(\omega)|\mathbf{E}_n(r')|^2\right] \tag{10}$$

$\phi_A(\omega)$ does not exactly follow the Lorentzian line shape when the materials are dispersive. Nevertheless, for the cases that σ_A and σ_E do not abruptly vary at $\omega \approx \mathrm{Re}[\omega_n]$, $\psi_A(\omega) \approx \psi_A(\mathrm{Re}[\omega_n])$ indicates the peak of the near-field energy transfer power density. Equation 10 alone fails to describe the dominant mechanism for maximizing the peak value $\psi_A(\omega)$ and, thus, guide the emitter design. Here, we further express $\mathrm{Im}[\omega_n]$ using the resonant modes $[\mathbf{E}_n(r), \mathbf{H}_n(r)]$. From eq 6, it has the mathematical identity $\int_{\partial V}\mathrm{d}r^2[\mathbf{E}_n \times \mathbf{H}_n^\dagger + \mathbf{E}_n^\dagger \times \mathbf{H}_n] = -2\int_V \mathrm{d}r^3(|\mathbf{H}_n|^2\mathrm{Im}[\omega_n]\mu_0 + |\mathbf{E}_n|^2\mathrm{Im}[\omega_n\epsilon(\omega_n)])$, where V is the volume enclosed by ∂V (as shown in Figure 1), and $\mathrm{Im}[\omega_n\epsilon(\omega_n)] = \sigma(\mathrm{Re}[\omega_n]) + \mathrm{Im}[\omega_n]\mathrm{Re}\left[\frac{\partial\omega\epsilon}{\partial\omega}\Big|_{\omega=\mathrm{Re}[\omega_n]}\right] + o(\mathrm{Im}[\omega_n]^2)$. As a result, $\mathrm{Im}[\omega_n]$ can be expressed as

$$\frac{1}{-\mathrm{Im}[\omega_n]} \approx \frac{\frac{1}{2}\int_V \mathrm{d}r^3\left[\mathrm{Re}\left(\frac{\partial\omega\epsilon(r,\omega)}{\partial\omega}\right)_{\mathrm{Re}[\omega_n]}|\mathbf{E}_n|^2 + \mu_0|\mathbf{H}_n|^2\right]}{\int_{\partial V}\mathrm{d}r^2\frac{1}{2}\mathrm{Re}[\mathbf{E}_n \times \mathbf{H}_n^\dagger] + \int_{V_E+V_A}\mathrm{d}r^3\frac{1}{2}\sigma(\mathrm{Re}[\omega_n])|\mathbf{E}_n|^2} \tag{11}$$

Equation 11 agrees with the conventional definition of the mode loss rate $\tau = -1/\mathrm{Im}[\omega_n]$, which equals the energy stored in the resonator divided by the energy loss per cycle.[18] In addition, the numerator on the right-hand-side (RHS) of eq 11 agrees with the universal description of the energy density, especially in the dispersive materials like metal.[23] Substituting eq 11 into eq 10, the peak value of the near-field spectral energy transfer from V_E to V_A equals

$$\Psi_A = 4\left(\frac{D_E}{D_E + D_A + D_\infty}F\right)\left(\frac{D_A}{D_E + D_A + D_\infty}F\right) \tag{12}$$

where $D_E = \int_{V_E}\mathrm{d}r^3\frac{1}{2}\sigma_E(\mathrm{Re}[\omega_n])|\mathbf{E}_n(r)|^2$ and $D_A = \int_{V_A}\mathrm{d}r^3\frac{1}{2}\sigma_A(\mathrm{Re}[\omega_n])|\mathbf{E}_n(r)|^2$ represent the mode energy losses due to the resistive dissipation in the emitter and the absorber, respectively. $D_\infty = \int_{\partial V}\mathrm{d}r^2\frac{1}{2}\mathrm{Re}[\mathbf{E}_n(r) \times \mathbf{H}_n^\dagger(r)]$ has the form of the mode energy loss due to far-field radiation. F is a factor attributed to the non-Hermitian imperfection of the lossy resonant mode expansion, which equals $F = \left|\int_V \mathrm{d}r^3\left\{\mathrm{Re}\left[\frac{\partial\omega\epsilon}{\partial\omega}(\mathrm{Re}[\omega_n])\right]|\mathbf{E}_n|^2 + \mu_0|\mathbf{H}_n|^2\right\}\right| / |N_{nn}|$.

Next, we investigate the far-field thermal radiation of V_E in eq 5 with the substitution of eqs 7 and 8. For the frequency ω close to the resonant frequency $\mathrm{Re}[\omega]$ of the mode, the first term on the RHS of eq 5 becomes

$$4\omega\mu_0\mathrm{Tr}\left[\int_{V_E}\mathrm{d}r^3\sigma_E\mathrm{Im}[\bar{\mathbf{G}}_{\omega,r,r}]\right] \approx 4\mathrm{Im}\left[\frac{1}{(\omega_n - \omega)}\right]\mathrm{Re}\left[\frac{\int_{V_E}\mathrm{d}r^3\sigma_E(\omega)\mathbf{E}_n(r)^T\mathbf{E}_n(r)}{N_{nn}}\right] = L(\omega)\psi_1(\omega) \tag{13}$$

where the peak value $\Psi_1 = \psi_1(\mathrm{Re}[\omega_n]) = 4\left(\frac{D_E}{D_E + D_A + D_\infty}F\right)P$, and the factor P is defined as

$$P = \mathrm{Re}\left[\frac{\int_{V_E}\mathrm{d}r^3\sigma_E\mathbf{E}_n(r)^2}{N_{nn}}\right] \Big/ \frac{\int_{V_E}\mathrm{d}r^3\sigma_E|\mathbf{E}_n(r)|^2}{|N_{nn}|} \tag{14}$$

where $\mathbf{E}_n^2 = \mathbf{E}_n^T \cdot \mathbf{E}_n$. P is the other imperfection factor due to the non-Hermitian fact as compared to the factor F. Mathematically, it has $P \le 1$. Since the second and the third terms in eq 5 have the same form with eq 4, the spectral thermal radiation of V_E to far-field can be derived from eqs 12 and 13 as $\phi_\infty(\omega) = \frac{\Theta}{2\pi}L(\omega)\psi_\infty(\omega)$, where the peak value $\Psi_\infty = \psi_\infty(\mathrm{Re}[\omega_n])$ equals

$$\Psi_\infty = 4\left(\frac{D_E}{D_E + D_A + D_\infty}F\right)\left(P - \frac{D_E + D_A}{D_E + D_A + D_\infty}F\right) \tag{15}$$

Hence, eqs 12 and 15 represent a new theoretical framework to understand and control the thermal radiation from optical

DOI: 10.1021/acsphotonics.7b00336
ACS Photonics 2017, 4, 1552−1557

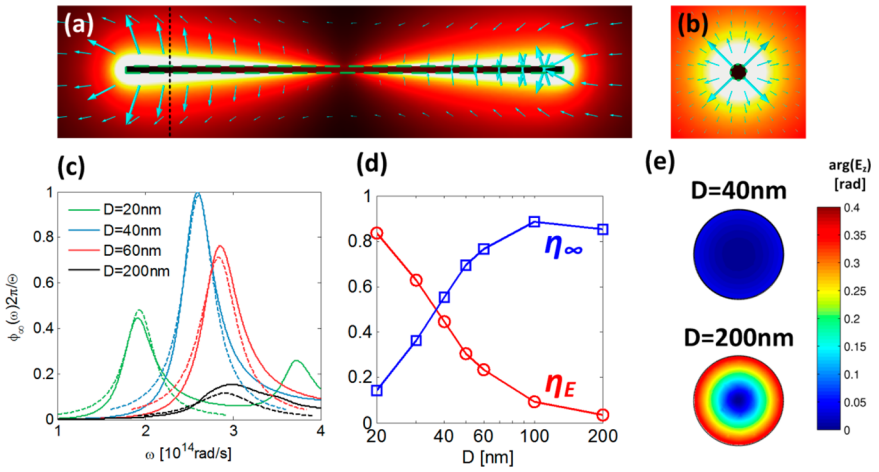

Figure 2. (a, b) Electric field profiles of the fundamental resonant mode of the gold nanorod with D = 40 nm and L = 2.5 μm. The color profile and the arrows indicate the field intensity and polarization, respectively. (c) Spectral energy flux of thermal emission evaluated based on our theory (dash curves) and direct calculation (solid curves). (d) Fractional mode losses for the cases with different D. (e) Electric field phase profile of the resonant mode in the cross-section of the gold nanorod.

resonators in both near- and far-fields. To interpret the weights of the mode energy losses into all possible sources, we define the fractional mode losses of the emitter, the near-field absorber, and the far-field as $\eta_E = \frac{D_E}{D_E + D_A + D_\infty}F$, $\eta_A = \frac{D_A}{D_E + D_A + D_\infty}F$ and $\eta_\infty = P - \eta_E - \eta_A$, respectively. Although the values of D_∞ and F depend on the choices of the enclosure surface ∂V and the volume V, η_E, η_A, and η_∞ all have fixed values because $\frac{F}{D_E + D_A + D_\infty} = \left|\frac{4}{\mathrm{Im}[\omega_n]N_{nn}}\right|$ according to eq 11. As a result, eqs 12 and 15 become

$$\Psi_A = 4\eta_E\eta_A$$
$$\Psi_\infty = 4\eta_E\eta_\infty \quad (16)$$

given that both Ψ_A and Ψ_∞ are positive, and $\eta_E + \eta_A + \eta_\infty = P$, the maxima of both Ψ_A and Ψ_∞ are equal to P^2, when $\eta_E = \eta_A = \frac{P}{2}$ and $\eta_\infty = 0$ for near-field thermal radiation, and $\eta_E = \eta_\infty = \frac{P}{2}$, $\eta_A = 0$ for far-field thermal radiation.

Because of the modulation of a single resonant mode, both near-field and far-field spectral thermal energy fluxes follow the Lorentzian line shape. To maximize thermal emission, eqs 12 and 15 demonstrate that the fractional mode losses must be matched in order to achieve maximized thermal radiation, that is, $\eta_E = \eta_A = \frac{P}{2}$ for near-field emission, and $\eta_E = \eta_\infty = \frac{P}{2}$ for far-field emission. In our theory, the peak or maximum value of both near-field and far-field spectral thermal emission equals $\frac{\Theta}{2\pi}P^2$, which is the key distinction from coupled-mode theory, that is, the peak value equals $\frac{\Theta}{2\pi}$.[16,17] To maximize P for reaching the limit of the peak value, eq 14 suggests that optical resonator thermal emitters can be designed to have electrical quasi-static resonant modes, that is, the electric field oscillates in phase. In this case, we prove $P \approx 1$ and $F \approx 1$ because (i) by choosing V to only enclose the near-field components of the resonant mode, the portion of the resonant mode outside V behaves as the propagating waves and therefore $\left(\frac{\partial\omega\epsilon}{\partial\omega}\right)\mathbf{E}_n^2 = \epsilon\mathbf{E}_n^2 \approx \mu\mathbf{H}_n^2$, which results in $N_{nn} \approx \int_V \mathrm{d}r^3\left(\frac{\partial\omega\epsilon}{\partial\omega}\right)\mathbf{E}_n^2 - \mu\mathbf{H}_n^2$; (ii) the portion of the resonant mode inside V behaves to be quasi-static, where $\mathbf{H}_n = \frac{1}{i\omega\mu_0}\nabla\times\mathbf{E}_n \approx 0$ and, thus, $N_{nn} \approx \int_V \mathrm{d}r^3\left(\frac{\partial\omega\epsilon}{\partial\omega}\right)\mathbf{E}_n^2$; (iii) Since the quasi-static electric field has a real value, $\int_{V_E}\sigma_E\mathbf{E}_n^2 \approx \int_{V_E}\sigma_E|\mathbf{E}_n|^2$ and $N_{nn} \approx \int_V \mathrm{d}r^3\left(\frac{\partial\omega\epsilon}{\partial\omega}\right)|\mathbf{E}_n^2| \approx |N_{nn}|$ based on the fact $\frac{\partial\omega\epsilon}{\partial\omega} > 0$. Likewise, $F \approx \left|\frac{\int_V \mathrm{d}r^3\mathrm{Re}\left[\frac{\partial\omega\epsilon}{\partial\omega}\right]|\mathbf{E}_n|^2}{\int_V \mathrm{d}r^3\left(\frac{\partial\omega\epsilon}{\partial\omega}\right)\mathbf{E}_n^2}\right| \approx 1$. As a result, in the quasi-static condition, our formalism agrees with coupled mode theory but has the direct electromagnetic definition for each mode energy loss.

Far-Field Thermal Emission. In order to validate our formalism, we investigate the far-field and near-field thermal emission spectra of the optical resonators made from metal nanorods, where the theoretical predictions by eqs 12 and 15 are compared with the direct simulations by the Fluctuating-Surface Current (FSC) method.[6,24] The field profile and the eigen-frequency of the lossy resonant modes are numerically calculated by the fully vectorial finite-element method,[21] and the fractional mode losses η_E, η_A, and η_∞ can then be evaluated accordingly.

Consider the far-field thermal radiation of a gold nanorod in the spectral range corresponding to its fundamental resonant modes (Figures 2a,b), which is indeed the Fabry–Perot resonance of the TM_0 waveguding mode. The length of the nanorods is kept as L = 2.5 μm, and the material is chosen to have a Drude model with $\omega_p = 1.37 \times 10^{16}$ rad·s^{-1} and $\gamma = 5.32 \times 10^{13}$ rad·s^{-1}. The predicted and the simulated emission spectra of the nanorods with different diameters D are plotted in Figure 2c. The good agreement between our predictions and the direct simulations convincingly verifies our formalism in the far-field case. Figure 2d further investigates the values of η_E and η_∞ at different diameters D. The monotonic increase of η_E is attributed to the fact that the dissipative loss of the TM_0 waveguiding mode increases as the decrease of the waveguide lateral size D.[25] At $D \sim 40$ nm, the radiative and the resistive mode losses are matched, and meanwhile, $P \to 1$, that is, $\eta_E = \eta_\infty \sim 0.5$. Consequently, the thermal emission peak reaches to the theoretical limit $\frac{\Theta}{2\pi}$. According to our aforementioned proof,

DOI: 10.1021/acsphotonics.7b00336
ACS Photonics 2017, 4, 1552–1557

the reason for $P \rightarrow 1$ at $D \sim 40$ nm is that the electric field of the resonant mode inside the metal nanorod is approximately quasi-static with the uniform phase, as shown in Figure 2e. However, for a thick nanorod, for example, $D = 200$ nm, the phase of the electric field varies significantly in the cross sections and consequently $P = 0.9 < 1$.

Near-Field Thermal Emission. Next, we investigate the near-field radiative transfer between two gold nanorods separated by a distance of 50 nm. By calculating the fundamental resonant mode in Figures 3a,b, the energy transfer

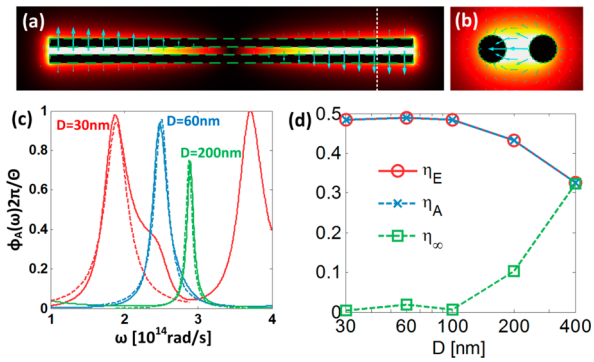

Figure 3. (a, b) Electric field profiles of the fundamental resonant mode of two aligned gold nanorods with $D = 60$ nm, $L = 2.5$ μm, and a 50 nm gap. Color profile and the arrows indicate the field intensity and polarization, respectively. (c) Spectral energy flux of thermal emission evaluated based on our theory (dash curves) and direct calculation (solid curves). (d) Fractional mode losses for the cases with different D.

spectra at different diameters D are predicted in Figure 3c, which agree well with the direct simulation results and therefore our formalism in the near-field case is also verified. The "bump" around the first peak of red curve in Figure 3c is attributed to a degenerate "symmetric" mode, while the "antisymmetric" mode makes major contribution to the energy loss channel. Figure 3d plots the fractional mode losses at different D, where $\eta_E = \eta_A$ is because the emitter and the absorber are exactly the same, and $\eta_E = \eta_A \rightarrow 0.5$ for $D \rightarrow 0$ is due to the same reason as that of the single nanorod cases, that is, the dissipative loss of the TM_0 waveguiding mode is monotonically increasing as the decrease of the lateral size. Overall, our theory can well predict both far-field and near-field thermal radiation spectra under the assumption of single predominant resonance mode. In general, this assumption is valid if (i) the resonance modes of the structure have distinct resonance frequencies; and (ii) the resonance mode accounts for the major energy decay channel of thermal radiation, which implies that a significant portion of the mode field profile is concentrated around the emitter,[14] as shown in Figures 2a and 3a from the finite-element-method (FEM) calculations. In addition, the small deviation between our theory and the direct simulations in Figures 2c and 3c is mainly because the nonresonance contribution to thermal radiation is ignored in our theory. For a lossy system like thermal emitter, the expansion of the dyadic Green's function into the quasi-normal modes in eq 7 approximately holds, where rigorously, a nonresonance noise term needs to be added to the RHS of eq 7. Such a nonresonance term can cause the slight deviation of our theory from the actual value, especially when the resonance mode is less predominant.

Finally, we propose to employ densely packed optical resonators to build meta-surface based near-field thermal emitters with monochromatic and super-Planckian emission. Since the resonance mode of a thermal resonator coupled to a proximal absorber can highly confine the electromagnetic field in a very small volume (Figure 3b), densely packed optical resonators on a surface create a large number of degenerated resonance modes in a unit area as long as the adjacent resonators have the weak interaction, and therefore, the overall energy flux can be estimated as $\Phi \approx \int \frac{d\omega}{2\pi} \Delta\Theta\left[\frac{1}{A}\phi_I(\omega)\right]$, where $\phi_I(\omega)$ is the energy flux due to an individual resonator, A is the lateral area occupied by a unit cell. In comparison with the blackbody limit $\Phi_{BB} = \int \frac{d\omega}{2\pi} \Delta\Theta\left(\frac{2\pi}{\lambda^2}\right)$,[26] we have $\Phi \gg \Phi_{BB}$ for the cases of $A \ll \lambda^2$. To prove the concept, we directly calculate the near-field energy transfer between two aligned densely packed gold nanorod arrays with $A = 3$ μm $\times$ 0.5 μm (Figure 4a) by the Wiener-Chaos-Expansion method.[27] In Figure 4b,

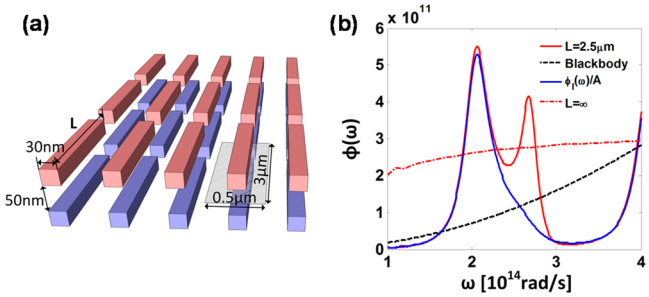

Figure 4. (a) Schematic of the meta-surface based thermal emitter and absorber made from densely packed nanorods and (b) spectra of near-field energy transfer.

the peak of the spectral energy flux at $\omega = 2.1 \times 10^{14}$[rad/s] is 1 order of magnitude larger than the blackbody radiation limit, and $\Phi \sim 2\Phi_{BB}$ when the temperatures of the emitter and the absorber are 500 and 0 K, respectively. Note that the periodicity of the nanorods in Figure 4a is not necessary because the energy is transferred in a pairwise manner, which can be further proven by the fact that the estimated spectrum $\frac{1}{A}\phi_I(\omega)$ agrees well with the actual energy flux spectrum near the main peak, as shown in Figure 4b. The smaller spectral heat flux peak adjacent to the major peak emerges when densely packing the optical resonators, which can be attributed to the Fano resonance effect. In the case of emitter arrays, the scattering field from the structure can be greatly enhanced by the interaction between adjacent nanorod emitters which may provide more pronounced constructive or destructive interference between the scattering and the resonant fields.

Our method for realizing super-Planckian near-field thermal emission is intrinsically different from the well-known approach by introducing a large number of degenerate modes.[28] We perform the 2D FSC direct calculation to further demonstrate the spectral near-field energy transfer of two nanorod arrays can exceed that of two infinite-long nanowire arrays by setting $L \rightarrow \infty$ (Figure 4a), where the near-field energy transfer of two infinite-long nanowire arrays is modulated by the propagating transmission line modes. In most cases, the temperature T and the Planck's distribution $\Theta(\omega, T)$ is not important for the design of narrow-band thermal radiation since the line-shape of the resonance peak is only slightly modified by $\Theta(\omega, T)$.

DOI: 10.1021/acsphotonics.7b00336
ACS Photonics 2017, 4, 1552−1557

Although the near-field energy flux of optical resonator based meta-surfaces may be weaker than the cases of hyperbolic metamaterials and the ultimate theoretical limit,[29] the tunable monochromatic spectrum demonstrates promising potential in developing highly efficient thermophotovoltaics devices, since the thermal emission peak frequency can be fully engineered to match the absorption bandgap of photovoltaic cells.[30,31]

In conclusion, we develop a general formalism from the fluctuational electrodynamics and quasi-normal mode theory to elucidate the underlying physics of the far-field and near-field thermal radiation from the optical resonators made by lossy and dispersive material. Because of the modulation from the resonant mode, the thermal emission power density spectrum of the optical resonators is narrow-band and follows the Lorentzian line shape with the peak at the resonant frequency of the mode. To maximize the thermal emission, our formalism demonstrates that not only the mode losses to the emitter and the absorber (or far-field background) require to be matched, but the resonant mode also needs to be electrically quasi-static, that is, the electric field of the resonant mode oscillates in phase. In addition, we validate our formalism by investigating the far-field and near-field thermal emission from metal nanorods. Our formalism can therefore serve as a general theoretical framework to design the narrow-band thermal emission of arbitrary resonant structures.

AUTHOR INFORMATION

Corresponding Author

*E-mail: sshen1@cmu.edu.

ORCID

Jiayu Li: 0000-0002-4759-2010

Sheng Shen: 0000-0002-9951-0814

Notes

The authors declare no competing financial interest.

ACKNOWLEDGMENTS

The authors acknowledge funding support from the U.S. National Science Foundation (CBET-1253692).

REFERENCES

(1) Inoue, T.; De Zoysa, M.; Asano, T.; Noda, S. Realization of Narrowband Thermal Emission with opti[1] T. Inoue, M. De Zoysa, T. Asano, S. Noda, Optica 2015, 2, 27.cal Nanostructures. *Optica* **2015**, *2*, 27−35.

(2) Lenert, A.; Bierman, D. M.; Nam, Y.; Chan, W. R.; Celanovic, I.; Wang, E. N. A Nanophotonic Solar Thermophotovoltaic Device. *Nat. Nanotechnol.* **2014**, *9*, 126−130.

(3) Basu, S.; Zhang, Z. M.; Fu, C. J. Review of near-Field Thermal Radiation and Its Application to Energy Conversion. *Int. J. Energy Res.* **2009**, *33*, 1203−1232.

(4) Raman, A. P.; Anoma, M. A.; Zhu, L.; Rephaeli, E.; Fan, S. Passive Radiative Cooling below Ambient Air Temperature under Direct Sunlight. *Nature* **2014**, *515*, 540.

(5) Otey, C. R.; Lau, W. T.; Fan, S. Thermal Rectification through Vacuum. *Phys. Rev. Lett.* **2010**, *104*, n/a.

(6) Liu, B.; Liu, Y.; Shen, S. Thermal Plasmonic Interconnects in Graphene. *Phys. Rev. B: Condens. Matter Mater. Phys.* **2014**, *90*, 195411.

(7) Schuller, J. A.; Taubner, T.; Brongersma, M. L. Optical Antenna Thermal Emitters. *Nat. Photonics* **2009**, *3*, 658−661.

(8) Liu, X.; Tyler, T.; Starr, T.; Starr, A. F.; Jokerst, N. M.; Padilla, W. J. Taming the Blackbody with Infrared Metamaterials as Selective Thermal Emitters. *Phys. Rev. Lett.* **2011**, *107*, n/a.

(9) Ghebrebrhan, M.; Bermel, P.; Yeng, Y. X.; Celanovic, I.; Soljačić, M.; Joannopoulos, J. D. Tailoring Thermal Emission via Q Matching of Photonic Crystal Resonances. *Phys. Rev. A: At., Mol., Opt. Phys.* **2011**, *83*, 33810.

(10) Thongrattanasiri, S.; Koppens, F. H. L.; García De Abajo, F. J. Complete Optical Absorption in Periodically Patterned Graphene. *Phys. Rev. Lett.* **2012**, *108*, 1−5.

(11) Novotny, L.; Hecht, B. *Principles of Nano-Optics*, 2nd ed.; Cambridge University Press, 2012.

(12) Rytov, S. M.; Kravtsov, Y. A.; Tatarskii, V. I. *Principles of Statistical Radiophysics*; Springer-Verlag, 1989; Vol. 3.

(13) Kristensen, P. T.; Hughes, S. Modes and Mode Volumes of Leaky Optical Cavities and Plasmonic Nanoresonators. *ACS Photonics* **2014**, *1*, 2−10.

(14) Sauvan, C.; Hugonin, J. P.; Maksymov, I. S.; Lalanne, P. Theory of the Spontaneous Optical Emission of Nanosize Photonic and Plasmon Resonators. *Phys. Rev. Lett.* **2013**, *110*, n/a.

(15) Ching, E. S. C.; Leung, P. T.; Van Den Brink, A. M.; Suen, W. M.; Tong, S. S. Quasinormal-Mode Expansion for Waves in Open Systems. *Rev. Mod. Phys.* **1998**, *70*, 1545−1554.

(16) Zhu, L.; Sandhu, S.; Otey, C.; Fan, S.; Sinclair, M. B.; Luk, T. S. Temporal Coupled Mode Theory for Thermal Emission from a Single Thermal Emitter Supporting Either a Single Mode or an Orthogonal Set of Modes. *Appl. Phys. Lett.* **2013**, *102*, 103104.

(17) Karalis, A.; Joannopoulos, J. D. Temporal Coupled-Mode Theory Model for Resonant near-Field Thermophotovoltaics. *Appl. Phys. Lett.* **2015**, *107*, 1−6.

(18) Jackson, J. D. *Classical Electrodynamics*; Wiley, 1998.

(19) Davies, E. B.; Davies, E. B. *Spectral Theory and Differential Operators*; Cambridge University Press, 1996; Vol. 42.

(20) Sauvan, C.; Hugonin, J. P.; Carminati, R.; Lalanne, P. Modal Representation of Spatial Coherence in Dissipative and Resonant Photonic Systems. *Phys. Rev. A: At., Mol., Opt. Phys.* **2014**, *89*, n/a.

(21) Bai, Q.; Perrin, M.; Sauvan, C.; Hugonin, J.-P.; Lalanne, P. Efficient and Intuitive Method for the Analysis of Light Scattering by a Resonant Nanostructure. *Opt. Express* **2013**, *21*, 27371.

(22) Ge, R.; Kristensen, P. T.; Young, J. F. Quasinormal Mode Approach to Modelling Light- Emission and Propagation in Nanoplasmonics. *New J. Phys.* **2014**, *16*, 113048.

(23) Landau, L. D.*Electrodynamics of Continuous Media*; Pergamon, 1984.

(24) Rodriguez, A. W.; Reid, M. T. H.; Johnson, S. G. Fluctuating-Surface-Current Formulation of Radiative Heat Transfer: Theory and Applications. *Phys. Rev. B: Condens. Matter Mater. Phys.* **2013**, *88*, 54305.

(25) Gacemi, D.; Mangeney, J.; Colombelli, R.; Degiron, A. Subwavelength Metallic Waveguides as a Tool for Extreme Confinement of THz Surface Waves. *Sci. Rep.* **2013**, *3*, 1369.

(26) Siegel, R. *Thermal Radiation Heat Transfer*, 4th ed.; Taylor & Francis, 2001.

(27) Liu, B.; Shen, S. Broadband near-Field Radiative Thermal Emitter/absorber Based on Hyperbolic Metamaterials: Direct Numerical Simulation by the Wiener Chaos Expansion Method. *Phys. Rev. B: Condens. Matter Mater. Phys.* **2013**, *87*, 115403.

(28) Biehs, S. A.; Rousseau, E.; Greffet, J. J. Mesoscopic Description of Radiative Heat Transfer at the Nanoscale. *Phys. Rev. Lett.* **2010**, *105*, 234301.

(29) Miller, O. D.; Johnson, S. G.; Rodriguez, A. W. Shape-Independent Limits to Near-Field Radiative Heat Transfer. *Phys. Rev. Lett.* **2015**, *115*, 204302.

(30) Greffet, J.-J.; Carminati, R.; Joulain, K.; Mulet, J.-P.; Mainguy, S.; Chen, Y. Coherent Emission of Light by Thermal Sources. *Nature* **2002**, *416*, 61−64.

(31) Narayanaswamy, A.; Chen, G. Surface Modes for near Field Thermophotovoltaics. *Appl. Phys. Lett.* **2003**, *82*, 3544.

DOI: 10.1021/acsphotonics.7b00336
ACS Photonics 2017, 4, 1552−1557